NANO LETTERS

2008
Vol. 8, No. 5
1532-1538

Analysis of the Vapor–Liquid–Solid Mechanism for Nanowire Growth and a Model for this Mechanism

S. Noor Mohammad[†]

Department of Materials Science and Engineering, University of Maryland, College Park, Maryland 20742

Received November 14, 2007; Revised Manuscript Received February 1, 2008

ABSTRACT

The vapor–liquid–solid (VLS) mechanism is most widely employed to grow nanowires (NWs). The mechanism uses foreign element catalytic agent (FECA) to mediate the growth. Because of this, it is believed to be very stable with the FECA-mediated droplets not consumed even when reaction conditions change. Recent experiments however differ, which suggest that even under cleanest growth conditions, VLS mechanism may not produce long, thin, uniform, single-crystal nanowires of high purity. The present investigation has addressed various issues involving fundamentals of VLS growth. While addressing these issues, it has taken into consideration the influence of the electrical, hydrodynamic, thermodynamic, and surface tension effects on NW growth. It has found that parameters such as mesoscopic effects on nanoparticle seeds, charge distribution in FECA-induced droplets, electronegativity of the droplet with respect to those of reactive nanowire vapor species, growth temperature, and chamber pressure play important role in the VLS growth. On the basis of an in-depth analysis of various issues, a simple, novel, malleable (SNM) model has been presented for the VLS mechanism. The model appears to explain the formation and observed characteristics of a wide variety of nanowires, including elemental and compound semiconductor nanowires. Also it provides an understanding of the influence of the dynamic behavior of the droplets on the NW growth. This study finds that increase in diameter with time of the droplet of tapered nanowires results primarily from gradual incorporation of oversupplied nanowire species into the FECA-mediated droplet, which is supported by experiments. It finds also that optimum compositions of the droplet constituents are crucial for VLS nanowire growth. An approximate model presented to exemplify the parametric dependency of VLS growth provides good description of NW growth rate as a function of temperature.

Introduction. Nanowires (NWs)[1–5] from semiconductors, particularly those[6–8] from III−V nitride semiconductors,[9] are very promising for nanoscale devices. A vast majority of these nanowires is synthesized by the vapor–liquid–solid (VLS) mechanism,[1–5] which makes use of a foreign element catalytic agent (FECA) for NW nucleation. FECA is actually a nanoparticle or a nanocluster made of metal atoms. In the conventional VLS picture, the whole process is assumed to be very stable with the FECA-mediated droplets not consumed even when reaction conditions change. The NW diameter d_{NW} dictated by the droplet size is, therefore, very stable. Recent experiments,[10–13] however, demonstrate that these assumptions are false. For example, even under cleanest growth conditions, VLS mechanism may not produce long and uniform nanowires[10] of high purity at a temperature T. Rather it produces nanowires exhibiting droplets at the tips and having a variety of shapes and sizes (see Figure 1) including the shape of a cone (the droplet edge is much thicker than the substrate edge; see Figure 1, structure S1) or a needle (the NW is gradually thinned as it grows, and is pointed at the droplet edge, while thick at the substrate edge; see Figure 1, structure S3). Nanowires may have diameters different from those of the droplets, even when these diameters are uniform (see Figure 1, structure S2). Also, the NW length L_{NW} may be different. Further, to find FECA that fits the VLS growth of a certain nanowire is still challenging.[14] Au is widely used as a FECA for the VLS growth of a variety of nanowires. Although it has strong chemical inertness and thermal stability, it presents formidable contamination problems.[15] This is all the more remarkable given the fact that VLS growth has been studied for over 40 years. Our objective in this investigation is to address various issues involving VLS growth, to understand the influence of the dynamic behavior of the droplets on NW growth, and to try to present a simple, novel, malleable (SNM) model for the VLS mechanism.

Analysis. For analysis of the mechanism and precise description of the model, we assume that the nanowire to be grown is $X_pY_qZ_r$ (X, Y, and Z are NW elements, and p, q, and r are mole fractions, p, q, and r may be an integer, and one or two of them may be zero) nanowire. The growth

[†] E-mail: snmd@umd.edu, snmohammad2002@yahoo.com. Associated also with the U.S. Naval Research Laboratory, Electronic Science and Technology Division, Washington, DC 20375.

10.1021/nl072974w CCC: $40.75
Published on Web 04/02/2008

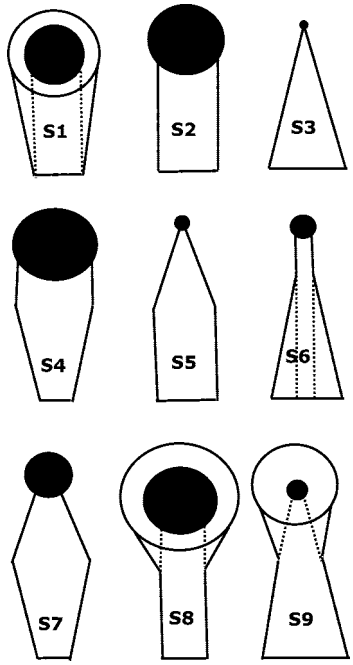

Figure 1. Schematic examples of possible nanowire structures formed under a variety of growth conditions. The structures S1, S2, and S3 are respectively cone shaped structure, uniform structure, and needle-shaped structure. Structures S4 to S9 are combinations of S1, S2, and S3 structures. In all the structures, the dark spherical droplets are made of FECA/X alloy. But in structures S1, S8, and S9, the outer peripheral segment (e.g., the one between the solid sphere and open sphere) of the droplet is due to integration of X into the droplet, which coexists with the FECA/X alloy as wetted nonalloyed component of the droplet. The nanowire segment of structures S1, S8, and S9 occurring between the solid line and dotted line is due to supersaturation and nucleation of $X_pY_qZ_r$ species through the nonalloyed component of the droplet. The nanowire segment of structures S6 occurring between the solid line and dotted line is due to diffusion of the FECA atoms or the R_S species from the substrate to the droplet via the NW sidewalls. The core (e.g., the one between two dashed line in the tapered region, and between two solid lines in the untapered region) of this nanowire is due to R_S species landing directly on the droplet surface.

can be done by techniques such as CVD, MBE, laser ablation, and microwave-assisted physical vapor transport where there are two zones: the high-temperature reaction zone and the low-temperature deposition zone. The substrate is placed in the deposition zone. The temperature T_H of the reaction zone is such that it produces X, Y, and Z vapor atoms either from the precursors or from solid sources of X, Y, and Z, respectively. The X, Y, and Z vapor atoms are then transported to the deposition zone by a suitable carrier gas, where they flow over a functionalized FECA-coated substrate placed inside a high vacuum furnace at temperature T_F and pressure P_L and produce, if not affected by oxygen or some other species, a FECA-induced droplet.

Central to the VLS mechanism are the formation, composition, overgrowth, and decay of droplets. Also, keys to the one-dimensional nucleation are surface tension and electronegativity of these droplets. These are described below. For VLS growth, T_F and P_L must be such that they cause FECA particles to form tiny alloyed seeds with that NW element (suppose X) for which the eutectic phase occurs at the lowest possible temperature T_E and with the lowest possible atomic percentage of X in the FECA/X composition C_L. The choice of T_F and P_L is indeed very critical. It must take into consideration the mesoscopic effect of the seeds. Because of this effect, there occurs melting point depression, and the melting point T_L at the tip of the seed can be far lower than that of the corresponding bulk. If the degree of temperature depression is T_M at pressure P_L, then T_L can be considerably lower[16] than the eutectic temperature T_E of the FECA/X binary phase diagram: $T_L = (T_E - T_M)$. Thus the tip of the seed can be a molten or semimolten alloy of composition C_L at T_L although T_L can be lower than T_E and T_F. Even when $T_L \approx T_F$, owing to the mesoscopic effect, the tiny tip of the seed may be molten/semimolten, with the rest of the substrate remaining as solid. The semimolten structure includes the one in which the seed may appear to be solid, and yet it has a lattice soft enough and interatomic/intermolecular configurations loose enough to allow the adsorption of the NW vapor species (e.g., X, Y, Z, etc.) on the droplet surface, and easy diffusion of these species from the droplet surface to the liquid/solid interface. While in the deposition zone, X, Y, and Z vapor atoms react to form $X_pY_qZ_r$ vapor molecules. More, and very likely, a majority of the $X_pY_qZ_r$ molecules are formed, however, when X, Y, and Z land on the droplet surface. These X, Y, and Z, together with the $X_pY_qZ_r$ vapor molecules, which land also on the droplet surface, participate in NW formation. $X_pY_qZ_r$, together with X, Y, and X are henceforth referred to as R_S species.

For the droplet to mediate NW growth, it must be such that the charge distribution Q_S and electrogenativity ζ_S of the R_S species (X, Y, Z, $X_pY_qZ_r$) are much different from the charge distribution Q_L and electronegativity ζ_L of the R_L species (e.g., droplet species including FECA/X alloy) of the droplet. An ideal FECA would be the one for which the difference $(\zeta_L - \zeta_S)$ creates a large electric field E. The FECA/X droplet should also have large surface tension γ_L. The electric field E and the surface tension γ_L must thus be sufficiently high for the R_S species to be attracted by the R_L species and to land on the droplet surface.

The molten FECA/X alloy, which is actually a liquid droplet of R_L species, should have low X composition C_L at temperature T_L. If the FECA/X droplet has very large fraction of X, then the difference $(\zeta_L - \zeta_S)$ may be too small for the $R_S \equiv X$, and even for the $R_S \equiv X_pY_qZ_r$ species, to land on the droplet surface. Low composition C_L of X in the R_L species is needed, as well, for smooth diffusion of $R_S \equiv X_pY_qZ_r$ through the droplet to the liquid–solid (L/S) interface. Note that this solid is the seed at the initiation of the growth, but is the NW tip (just underneath the droplet) in the subsequent stage of the growth.

Droplet overgrowth with time during NW growth is detrimental for VLS mechanism. It can occur due to continuous oversupply of the R_S species or the lack of control of relative flow rates of X, Y, Z vapor species in the deposition zone. If, for example, $R_S \equiv X$ vapor species, as compared to other vapor species, is flown excessively into

the deposition chamber, some of these $R_S \equiv X$ may be integrated into the droplet, partly changing the composition of the FECA/X alloy, or just coexisting with this alloy as wetted nonalloyed component of the droplet. The droplet size is consequently increased. Cone-shaped nanowires are produced when $X_pY_qZ_r$ molecules diffuse through the alloyed and nonalloyed segments of the droplet to the L/S interface. As shown in structures S1, S8, and S9 (see Figure 1), the peripheral region of the nanowire formed primarily by the nonalloyed component of the droplet, may actually be responsible for the gradual increase in NW diameter in the entire or certain section of the NW length.

Droplet decay and even disintegration with time during growth are also detrimental for the VLS mechanism. These can take place due to a number of reasons: First, there occurs a lateral temperature gradient and/or sudden change in temperature, which leads to accidental and random breakup of FECA droplets.[17] Second, oversupply of one or more R_S species, and interplay of surface energies of the nanowire and/or liquid droplet, result in droplet oscillation and multiple nucleation[17] during growth. Third, gas particles (carrier gases, R_S species, etc.) incident on the droplet surface can cause hydrodynamic stress χ_L (viscous and/or inertial) in the droplet. Obviously, χ_L is opposed by γ_L. While χ_L tends to deform the droplet from spherical to the ellipsoidal shape, reducing its surface energy, γ_L tends to preserve the spherical shape of the droplet. Thus, gas flow during NW growth can cause droplet breakup, and even droplet disintegration, if $\chi_L > \gamma_L$. Even when $\gamma_L > \chi_L$, some atoms from FECA particles located at the surface of the droplet, if hit hard by gas particles, may be knocked out and vaporized. It is particularly true at $T \gg T_L$ and $P \ll P_L$, at which the droplet is in a highly molten condition. That such breakup at high temperatures is possible is evident from the breakup of the water droplet by high-velocity gas flow.[18] Fourth, the droplets may be charged, for example, by tribo-electrification, ion collection, thermionic emission, frictional charging, etc. during growth. Example: Au nanoparticles, placed in tube furnace flowing high-purity nitrogen, became electrically charged[19] at $T > 600$ °C. Also, the decomposition of SiH_2Cl_2 during CVD growth produced charged silicon clusters.[20] So droplets become unstable and break apart if repulsive electrostatic forces on their surfaces exceed the surface tension forces.[21]

To reiterate, temperature T and pressure P play a crucial role in the droplet stability. Usually the higher the T above T_L and the lower the P below P_L, the higher is the degree of melting of the FECA/X alloy and the higher is the instability of the droplet. Atoms are more loosely bound in this alloy at higher T and lower P, and they (particularly those present near the surface) have a higher tendency to dissociate from the alloy under hydrodynamic stress or due to an impulse from incident charge particles. So, at an appropriate pressure P (generally 1−10 Torr), temperature T must be close to T_L, and that at this T (called T_B), the droplets should be stable, have high γ_L, exert high electric field on R_S species (X, Y, Z, $X_pY_qZ_r$), and allow smooth diffusion of $R_S \equiv X_pY_qZ_r$ species through it. At this pressure P, T_B should never be high enough, at which the droplets are highly unstable, or

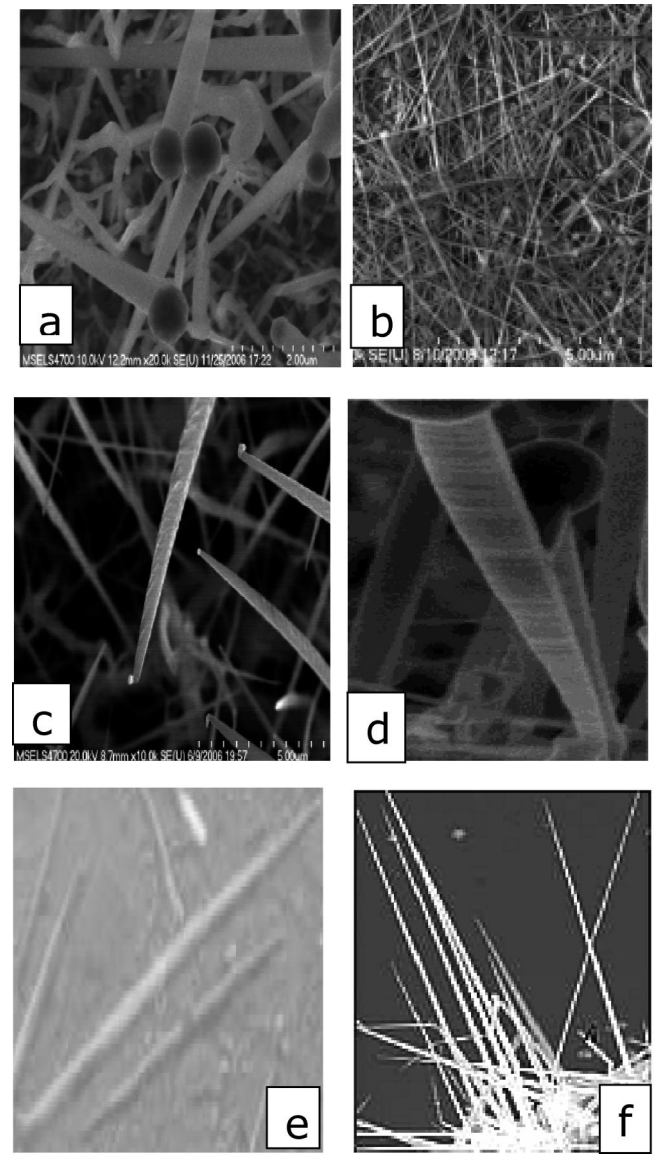

Figure 2. Examples of as-grown nanowires that resemble (a) cone-shaped structure S1, (b) uniform-structure S2, (c) needle-shaped structure S3, (d) hybrid structure S4 (e.g., combination of S1 and S2 structures), and (e) hybrid structure S7 (e.g., combination of S1 and S3 structures) and provide evidence of variations in NW structures under a variety of growth conditions. While the as-grown nanowires presented in (a,b,c) are SiC nanowires from Sundarasen et al.,,[22] the as-grown ZnO nanowire in (d) is from Gao and Wang.[23] The as-grown InN nanowires in (e) and (f) are from our laboratory.[27]

there occurs chemical reaction of FECA with the R_S species. If it happens, the droplet size would reduce with time during the entire or certain period of growth (see Figure 1, structures S3, S5, S7) and it may even disappear. Even if it exists, its chemical makeup, electronic charge distribution, surface tension, and the electronegativity can all alter leading to bending, twinning, splitting, etc. of nanowires. That the structures of Figure 1 resulting from various effects are indeed realistic is apparent from some as-grown nanowires[22,23] presented in Figure 2.

The NW growth rate depends on the diffusion length λ_{SD} of the R_S species. It is given by[24] $\lambda_{SD}^2 = D_{S0}\tau_S \exp(-\beta_{SD}E_{SD}/$

k_BT), where τ_S is the carrier lifetime, β_{SD} is a parameter, D_{S0} is the temperature-independent diffusion coefficient, k_B is the Boltzmann constant, and E_{SD} is the diffusion activation energy. On the basis of this equation, the diffusion length λ_{SD} is larger at higher temperature. This means the NW growth rate G_{NW} is higher if the NW growth can be conducted at higher temperature at least until G_{NW} reaches the peak. As this temperature, T_B should not be much higher than T_L. FECA, for a particular NW growth, should be so chosen[25] that the FECA/X alloy exhibits the highest possible T_L. Also, T_B corresponding to this T_L must be such that at $T \approx T_B$, G_{NW} is the highest, and the NW tapering due to sidewall migration of FECA or R_S species from the substrate is the lowest.

The eutectic temperature T_E is 363 °C for Au−Si (97% Au and 3% Si) alloy, is 450 °C for Au−In (68% Au and 32% In) alloy, and 1200 °C for Fe−Si (70% Fe and 30% Si) alloy. Hannon et al.[10] grew Au-catalyzed Si nanowires at T= 600 °C and $P = 5 \times 10^{-5}$ Torr. Cao et al.[12] grew Au-catalyzed Si nanowires at T = 500–700 °C and $P < 5$ Torr. Mattila et al.[11] grew Au-catalyzed InP (X = In, Y = P, $p = q = 1$, and $r = 0$) nanowires at T = 420−450 °C. Sundaresan et al.[22] grew Fe-catalyzed SiC (X = Si, Y = C, $p = q = 1$, and $r = 0$) nanowires by a microwave-assisted physical vapor transport process at atmospheric pressure. For this SiC NW growth, the difference in temperature, ΔT, between the reaction zone and the deposition zone was ∼150 °C, the distance between these two was ∼200 μm, and the duration of substrate heating was ∼15 s. However, the temperature T of the deposition zone was varied. Thus, cone-shaped nanowires, about 2−5 μm in length, were grown at $T \approx$ 1600 °C, needle-shaped nanowires, up to ∼100 μm in length, were grown at $T \approx$ 1700 °C, and nanowires of uniform diameters, about 10−30 μm in length and 15−300 nm in diameter, were grown at $T \approx$ 1650 °C. Only micrometer-sized SiC deposits could be obtained at $T >$ 1750 °C. The diameter of the cone shaped nanowires was 10−50 nm at the substrate end, but 100−200 nm at the tip. The diameter of the needle shaped nanowires was 10−50 nm at the substrate end and almost zero at the tip. All these are shown in Figure 2, and can be explained well by the present model, as detailed below.

There are three possible reasons for the growth of cone-shaped nanowires. First, there are some FECA particles in the vapor phase. Also, X, as compared to Y, Z, and $X_pY_qZ_r$ is oversupplied. ζ_S values for all R_S species (X, Y, Z, $X_pY_qZ_r$) and FECA are different from ζ_L, so all of them land (at constant rate with time) on the droplet surface under the influence of the electric field E and the surface tension γ_L. Some of these $R_S \equiv X$ form FECA/X alloy with FECA particles, others combine with Y and Z to create additional $X_pY_qZ_r$ molecules. The diameter of the droplet and the nanowire thus increase with time. Second, FECA atoms migrate from small-catalyst NW droplets to large-catalyst NW droplets to reduce the total droplet surface area, and this migration via diffusion takes place along NW sidewalls. Various R_S species (X, Y, Z, $X_pY_qZ_r$) land at the same time on the droplet surface. Some of the $R_S \equiv X$ atoms form FECA/X alloy with the surface migrated FECA, while others combine with Y and Z to create $X_pY_qZ_r$ molecules. Droplet and NW diameters are consequently increased with time. Third, there are no FECA atoms landing on or migrating to the droplet. Only R_S species (X, Y, Z, $X_pY_qZ_r$) land on the droplet surface. Some of these $R_S \equiv X$, if not very highly energetic, are integrated into the droplet, partly changing the composition of the FECA/X alloy or just coexisting with this alloy as a wetted nonalloyed peripheral component of the droplet. The droplet size is consequently increased with time. The remaining X atoms form $X_pY_qZ_r$ molecules with Y and Z atoms and the $X_pY_qZ_r$ molecules diffuse through the droplet to produce nanowires. That a nonalloyed droplet can indeed promote NW growth well is evident from the VLS-type self-catalytic NW growth carried out in our laboratory.[6–8]

Of the three possibilities, the third one appears to be most plausible for SiC nanowires grown at $T \approx$ 1600 °C under Si-rich conditions. It is supported by Novotny and Yu.[26] With $R_S \equiv$ Si continuing to be integrated into the droplet, the ζ_L of the FECA/X alloy approached the ζ_S of $R_S \equiv X$, and the difference ($\zeta_L - \zeta_S$) gradually decreased. At one point, it was too small for $R_S \equiv$ Si to land on the droplet surface where it could produce, together with C atoms, SiC molecules. With X = Si composition C_L being relatively large under Si-rich conditions at which T_E is possibly larger (T_E depends on the atomic percentage of Si; see for example, Wang et al., ref 16), $R_S \equiv$ SiC molecules primarily from the vapor phase could diffuse slowly through the droplet onto the L/S interface to produce nanowires. That these are correct is evident by very slow NW growth;[22] nanowires only 2−5 μm in length could be produced. Had the first or second option been true, nanowires would grow longer and have S1, S4, or S7 structures of Figure 1. Diffusion of Fe through NW sidewall from the substrate to the droplet, or vice versa, may be reasonable more for NW lengths smaller than 1 μm than for NW lengths larger than 1 μm. It may particularly be very unlikely[12] for the FECA particles to diffuse upstream to a length as large as 5 μm.

Nanowires of uniform diameters can be realized under the two following conditions: First, R_S species (X, Y, Z, and $X_pY_qZ_r$) land on the droplet surface (at constant rate with time), and there is no oversupply of any of the R_S species. Also, the droplet is sufficiently stable at the growth temperature and pressure to resist decay or disintegration by hydrodynamic stress or the impulse of charge particles, if any. Second, there is an oversupply of one of the R_S species (suppose X), but the temperature is high, and X species are energetic enough not to be wetted or integrated, at least in large number, into the droplet to increase the droplet size. Those that tend to be wetted and integrated into the droplets are counteracted by the hydrodynamic effect and/or the impulse of charged particles. A variety of nanowires (GaN, InAs, InGaAs, InGaN, InGaAsN, etc,) grown in our laboratory[6,7] followed the first condition. However, the uniform SiC nanowire grown at $T \approx$ 1650 °C by Sundaresan et al.[22] under Si-rich conditions appears to follow the second condition. $R_S \equiv$ SiC formed in the vapor phase, or formed

from Si and C on the droplet surface, diffused through the droplet to form nanowires shown in Figure 2b. The NW length was also considerably larger (10−30 μm)[22] but not significantly large due to somewhat larger value of C_L.

Needle-shaped nanowires are produced under one of the four following conditions: First, R_S species (X, Y, Z, and $X_pY_qZ_r$) land on the droplet surface (at constant rate with time), and there is no oversupply of any R_S species. However, the droplet is not sufficiently stable at the growth temperature and pressure to resist decay or disintegration by hydrodynamic stress or the impulse of charge particles. So, the droplet becomes gradually smaller as the nanowire grows. Second, there is gradual decrease in the supply of $R_S \equiv X_pY_qZ_r$ species with time to the droplet. Third, the growth temperature is high and the chamber pressure is quite low. The droplet is highly molten at this growth temperature $T \gg T_L$ and pressure $P \ll P_L$. So the droplet can no longer hold the R_L species, and particles from this R_L species diffuse from the droplet to the substrate via the NW sidewalls. Consequently, the droplet size is gradually reduced as the nanowire grows. Fourth, the growth temperature is high, and one or more of the R_S species react with FECA gradually, altering the very composition of the droplet alloy.

The first and second conditions (e.g., undersupply of In vapor) dominated needle-shaped InN nanowire growth in our laboratory.[6,27] Scattered metal particles[6] lying on the substrate surface (see Figure 2f) corroborate the suggestion that the loss of metal mass following the first condition does indeed take place. The third condition appears to dominate the Si nanowire growth by Hannon et al.[10] These nanowires grown at $T \gg T_L$ and $P \ll P_L$ had length smaller than 1 μm. The first and second conditions might have dominated the needle-shaped Si nanowire growth at $T \gg T_L$ but $P \approx P_L$ by Cao et al.[12] So, the droplets of Cao et al. were molten and unstable, but not near-liquefied as those of Hannon et al. Needle-shaped nanowires grown by Sundaresan et al.,[22] Cao et al.,[12] Kim et al.,[13] Zou et al.,[28] and in our laboratory[27] have lengths exceeding 10 μm, and these lengths are too long for downward NW surface diffusion to lead to gradual NW needling.

Needle-shaped SiC nanowires grown at $T \approx 1700$ °C (see Figure 2c) by Sundaresan et al.[22] were influenced by some or all of the above four conditions. At $T \approx 1700$ °C, the droplets were quite molten and unstable. So, highly energetic oversupplied Si vapor atoms were less likely to be integrated into the alloy. There was a possibility of two or more of Fe/Si alloy, Si, and C to react with each other as well. Interestingly, long nanowires ($\sim$100 μm) could still be grown because some Si atoms, rather than Fe atoms, were lost from Fe/Si alloy due to hydrodynamic effect and/or the effect of charge particles lowering C_L and easing the diffusion of $R_S \equiv$ SiC through the droplet in higher numbers. It was possible because the melting temperature of Si (1410 °C) is lower than that of Fe (1535 °C), and the boiling temperature of Si (2355 °C) is also lower than that of Fe (2750 °C).

Very high growth temperature can nullify NW growth. At this temperature, the droplet instability is too high and there can be chemical reactions between FECA and R_S species. During SiC nanowire growth at $T > 1700$ °C, chemical reactions[29] between the SiC and Fe such as Fe + SiC → Fe_3C + Fe(Si) and Fe + SiC → Fe_3Si + Fe_2Si + C might have played a dominant role. The droplets thus disintegrated, and only SiC deposits could be obtained.

Tapered, but not needled, nanowires (structure S6, Figure 1) grow under two different conditions: First, FECA atoms migrate from small-catalyst NW droplets to large-catalyst NW droplets via NW sidewalls to reduce the total droplet surface area, but the larger the NW length, the smaller is the number of FECA atoms reaching the droplet via the NW sidewalls. Suppose L_F is the largest NW length up to which the FECA atoms can migrate upward. Then the largest number of migrated FECA atoms integrates into the FECA/X alloy of the droplet when the nanowire length $L_{NW} \approx 0$ at the initiation of NW growth, but almost no FECA atoms can integrate into the FECA/X alloy of the droplet at $L_{NW} \approx L_F$. These nanowires are tapered up to $L_{NW} = L_F$ but thinner and uniform for $L_{NW} > L_F$. Second, FECA atoms migrating from small-catalyst NW droplets to large-catalyst NW droplets are insignificant. But, while some of the R_S species land on the droplet surface, others of them land on the substrate surface. The R_S species landing on the substrate then migrate to the droplet via NW sidewall. Among them, some X atoms integrate into the droplet, partly changing the composition of the FECA/X alloy or just coexisting with this alloy as a wetted nonalloyed peripheral component of the droplet. Other R_S species (remaining X, and also Y, Z, and $X_pY_qZ_r$) migrating from the substrate participate in the NW growth via both the alloyed and nonalloyed segments of the droplet. If L_S is the largest NW length up to which the R_S species can migrate upward, then these nanowires are tapered up to $L_{NW} = L_S$ but thinner and uniform for $L_{NW} > L_S$. The thinner and uniform segment of the nanowires is produced by R_S species landing directly on the droplet surface from the vapor phase. As both L_F and L_S decrease with increasing temperature[30] due to decreasing mobility at the NW sidewalls and increasing adatom crystallization on the substrate surface, tapered nanowires grown at higher temperatures should have smaller tapered lengths. That tapering indeed ends at $T \approx T_B$ is demonstrated by nanowires produced by Dayeh et al.[31] and Dick et al.[32]

The Au-catalyzed InP NW characteristics[11] are remarkably similar to the Fe-catalyzed SiC NW characteristics.[22] While grown at 420, 430, 440, and 450 °C, InP nanowires are respectively cone-shaped, uniform, needle-shaped, and almost disintegrated. A comparison of the Au-catalyzed cone-shaped InP nanowires of Mattila et al.[11] with the self-catalyzed cone-shaped InP nanowires of Novotny and Yu[26] strongly supports our argument that the cone shape of nanowires results primarily from gradual incorporation of oversupplied X element into the FECA/X droplet.

To exemplify the parametric dependence of NW growth, we briefly discuss the Au-catalyzed Si NW growth rate as a function of temperature. As Kikkawa et al.[33] suggested, this growth rate depends on many parameters, including decomposition of SiH_4 and supersaturation and crystallization of

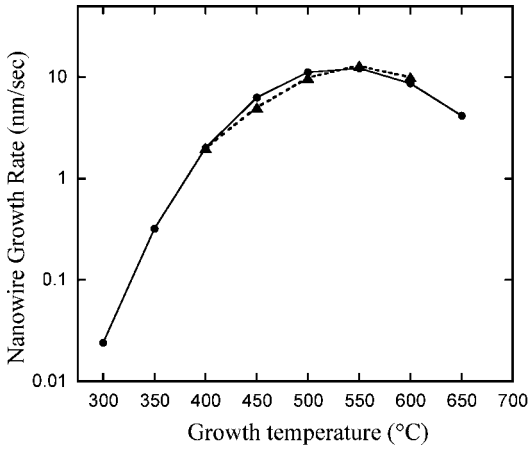

Figure 3. Comparison of the calculated results from our model with the experimental results from Lew and Redwing.[5] The solid line and the solid circles represent the calculated results. The dashed line and the solid triangles represent the experimental results.

the R_S species at the solid/liquid interface. According to Givargizov,[34] the supersaturation is given by $\xi = a(\mu_1 - \mu_2)/k_BT$, where μ_1 is the chemical potential in the vapor phase, μ_2 is the chemical potential in the solid phase, k_B is the Boltzmann constant, and a is a parameter that may depend on growth temperature, partial pressure of source gases, and the NW diameter d_{NW}. One may rewrite ξ as[35] $\xi = 2\omega\sigma(d_{NW} - d_{CNW})/(d_{NW}d_{CNW}k_BT)$, with ω as the atomic weight of the nanowire material, σ as the surface energy density of the nanowires, and d_{CNW} as the critical diameter of the nanowires. If expressed further in terms of the diffusion length, as done by Kikkawa et al., the growth rate may approximately be given by $G_{NW} = G_0 \exp(-\beta_{SD}E_{SD}/2k_BT)$, where $G_0 = a_0^2\xi_0^2(D_{S0}\tau_S)^{1/2}$, a_0 is a parameter, ξ_0 is the supersaturation of the NW species for nanowires of average diameter, and $\beta_{SD} = 4\cosh(T/T_B)$. We calculated G_{NW} for Si nanowires over the temperature range of 300–650 °C. For this calculation, we used $(D_{S0}\tau_S)^{1/2} = 100$ nm as given by Lim et al.,[36] $T_B \approx 400$ °C, as stated earlier, is the temperature at which the droplet is thermally stable, and the supersaturation for the Au-catalyzed Si reaches almost the peak, if not the peak, and $d_{CNW} = 1.8$ nm as given by Wilcoxon et al.[37] A comparison of the calculated results with available experiment of Lew and Redwing[5] is shown in Figure 3. This comparison is almost quantitative for $a_0\xi_0 = 1.3 \times 10^{17}/s^{1/2}$ and $E_{SD} = 150$ kJ/mol. G_{NW} increases with T until it reaches a peak and then decreases with increasing T. Thus, the model, although approximate, appears to be suitable enough to provide good description of the NW growth rate as a function of temperature.

Conclusion. In conclusion, analysis of the VLS mechanism has been presented. The analysis takes into consideration the influence of the electrical, hydrodynamic, thermodynamic, and surface tension effects on NW growth and provides better understanding of the VLS mechanism. A unified model based on this analysis appears to explain the formation of all sorts of nanowires. The analysis indicates that the difficulties encountered, for example, by Hannon et al. and Cao et al., in producing uniform nanowires arose from the lack of judicious choice of growth parameters. The arguments put forth by them seem to apply only to specific cases. This is evidenced by Hu et al.,[38] who used only 370 °C to produce Au-catalyzed uniform Si nanowires. The data of Hannon et al. and Cao et al., together with those by Sundaresan et al. and Mattila et al., are quite interesting and they provide strong justification to various features presented in our model. This model suggests that the VLS growth should preferably be performed at T not much higher than T_L. Otherwise, even the eutectic temperature T_E may prove to be too high for the stability of some droplets, particularly for those for which the depression temperature T_M is high. Any VLS growth must ensure that the composition of X in the FECA/X alloy is significantly low, the FECA does not contaminate the NW lattice structure, and the electric field E and the surface tension γ_L are high. This VLS growth must also ensure that the supply of various R_S species (X, Y, Z) is proportionately adequate, and the growth temperature and the chamber pressure are optimized enough to promote reaction among these R_S to produce $R_S \equiv X_pY_qZ_r$. Both the oversupply and undersupply of $R_S \equiv Y$ and/or $R_S \equiv Z$ may impede this reaction. The VLS growth may consequently be very slow. The VLS grown nanowires may also be affected if the cooling rate after NW growth is exceedingly high.

The presence of FECA at the tip of VLS grown nanowires leads to lattice disorder and defects. More importantly, it compromises the engineering applications of these nanowires. In general, the smaller the size of this FECA, the lower is the probability of such disorder and defect. Following the observation earlier, an important means to accomplish this goal, at least as much as possible, would be to introduce a growth technique in which the FECA/X alloy should be very small, and judiciously controlled oversupply of the $R_S \equiv X$ species would lead some of these X species to form wetted nonalloyed component of the droplet. This nonalloyed component of the droplet would actually be formed around the periphery of the FECA/X alloy of this droplet. And both of them would participate in NW growth. Recent experiments[37] indicate that indeed the formation of very tiny FECA/X nanoparticles with radii r_{CNW} as small as 0.85 nm is feasible. The nanowires of uniform diameter can thus be grown with the participation of both alloyed and nonalloyed components of the droplet in supersaturation and nucleation. These nanowires will have inner core, for example, of radius $r_{CNW} \approx 0.85$ nm and an outer shell of width w_{CNW}. The total NW radius would be $r_{NW} = r_{CNW} + w_{CNW}$, with w_{CNW} resulting from the participation of nonalloyed component of the droplet, and having a value quite variable depending upon need. Such nanowires would have homogeneous composition, desirable radii, and significantly lower defect level. Judicious control of growth temperature, chamber pressure, and relative supply of various R_S species with time would be very crucial for obtaining such uniform NW diameter.

Acknowledgment. The research is supported, in part, by DTRA Grant No. W911NF-06-1-0464 through the Army Research Office and monitored by Dr. Stephen Lee. The author thanks Dr. Albert V. Davydov and Siddarth Sundaresan for

illuminating discussions. Much of the present work reported in this article was carried out with the author being with Howard Univeristy, Washington, DC 20059.

References

(1) For reviews on nanowire science and technology, see: (a) Lauhon, L. J.; Gudiksen, M. S.; Lieber, C. M. *Philos. Trans. Roy. Soc. London, Ser. A* **2004**, *362*, 1247. (b) Lu, W.; Lieber, C. M. *J. Phys. D: Appl. Phys.* **2006**, *39*, R387. (c) Xia, Y. N.; Yang, P.; Sun, Y. G.; Wu, Y. Y.; Meyers, B. *Adv. Mater.* **2003**, *15*, 353. (d) Fan, H. J.; Werner, P.; Zacharias, M. *Small* **2006**, *2*, 700. (e) Teo, B. K. Sun, X.H. *Chem. Rev.* **2007**, *107*, 1454.

(2) Wagner, R. S.; Ellis, W. C. *Appl. Phys. Lett.* **1964**, *4*, 89.

(3) (a) Bartness, K. A.; Roshko, A.; Sanford, N. A.; Barker, J. M.; Davydov, A. V. *J. Cryst. Growth* **2006**, *287*, 522. (b) See also: Tham, D.; Nam, C.-Y.; Fischer, J. E. *Adv. Funct. Mater.* **2006**, *16*, 1197.

(4) Kryliouk, O.; Park, H. J.; Wang, H. T.; Kang, B. S.; Anderson, J. T.; Ren, F.; Pearton, S. J. *J. Vac. Sci. Technol., B* **2005**, *23*, 1891.

(5) Lew, K. K.; Redwing, J. M. *J. Cryst. Growth* **2003**, *254*, 14.

(6) (a) Mohammad, S. N. *J. Chem. Phys.* **2006**, *125*, 094705. (b) See also: He, M.; Mohammad, S. N. *J. Chem. Phys.* **2006**, *124*, 064714.

(7) (a) Mohammad, S. N. *J. Chem. Phys.* **2007**, *127*, 244702. (b) He, M.; Motayed, A.; Mohammad, S. N. *J. Chem. Phys.* **2007**, *126*, 064704.

(8) (a) He, M.; Fahmi, M. M. E.; Mohammad, S. N.; Jacobs, R. N.; Salamanca-Riba, L.; Felt, F.; Jah, M.; Sharma, A.; Lakins, D. *Appl. Phys. Lett.* **2003**, *82*, 3749. (b) See also: El Ahl, A. M. S.; He, M.; Zhou, P.; Harris, G.; Salamanca-Riba, L.; Felt, F.; Shaw, H.; Sharma, A. K.; Jah, M.; Lakins, D.; Steiner, D.; Mohammad, S. N. *J. Appl. Phys.* **2003**, *94*, 7749.

(9) (a) Mohammad, S. N. *Solid-State Electron.* **2002**, *46*, 203. (b) See also: Mohammad, S. N.; Morkoç, H. *Prog. Quantum Electron.* **1996**, *20*, 361.

(10) Hannon, J. B.; Kodambaka, S.; Ross, F. M.; and Tromp, R. M. *Nature* **2006**, *440*, 69.

(11) Mattila, M.; Hakkarainen, T.; Mulot, M.; Lipsanen, H. *Nanotechnology* **2006**, *17*, 1580.

(12) Cao, L.; Garipcan, B.; Atchison, J. S.; Ni, C.; Nabet, B.; Spanier, J. E. *Nano Lett.* **2006**, *6*, 1852.

(13) Kim, T. Y.; Kim, J. Y.; Lee, S. H.; Shim, H. W.; Lee, S. H.; Suh, E. K.; and Nahm, K. S. *Synth. Mater.* **2006**, *144*, 61.

(14) Nguyen, P. Ng, H. T. Meyyappan, M. *Adv. Mater.* **2005**, *17*, 1773. This article has presented an extensive discussion of the suitability of a certain FECA for a certain nanowire growth.

(15) Gu, G.; Burghard, M.; Kim, G. T.; Dusberg, P.; Chiu, P. W.; Krastic, V.; Roth, S.; Han, W. Q. *J. Appl. Phys.* **2001**, *90*, 5747.

(16) (a) Wang, Y. Schmidt, V. Senz, S. Gösele, U. *Nat. Nanotechnol.* **2006**, *1*, 186. (b) See also: Buffat, Ph; Borel, J. P. *Phys. Rev. A* **1976**, *13*, 2287; (c) Borel, J. P. *Surf, Sci.* **1981**, *106*, 1. These show that the melting point, for example, of Au nanoparticles (∼2 nm) can be lower by over 400 °C than the melting point of Au bulk material.

(17) Wagner, R. S., In *Whisker Technology*; Levitt, A. P., Ed.; John Wiley: New York, 1970.

(18) Stone, H. A. *Annu. Rev. Fluid Mech.* **1994**, *26*, 65.

(19) Magnussen, M. H.; Deppert, K.; Maln, J.; Bovin, J.; Samuelson, L. *J. Nanoparticle Res.* **1999**, *1*, 20.

(20) Hwang, M. M.; Jeon, I. D.; Kim, D. Y. *J. Ceram. Process. Res.* **2000**, *1*, 34.

(21) (a) Rayleigh, L. *Philos. Mag.* **1882**, *14*, 184. (b) Last, L.; Levy, Y.; Jortner, J. *Proc. Natl. Acad. Sci. U.S.A.* **2002**, *99*, 9107.

(22) Sundaresan, S. G.; Davydov, A. V.; Vaudin, M. D.; Levin, I.; Maslar, J. E.; Tian, Y.-L.; Rao, M. V. *Chem. Mater.* **2007**, *19*, 5531.

(23) (a) Gao, P.; Wang, Z. L. *J. Phys. Chem. B* **2002**, *106*, 12653. (b) See also: Sharma, S.; Sunkara, M. K.; Miranda, R. *Mater. Res. Soc. Symp. Proc.* **2001**, *676*, Y1.6.1.

(24) (a) Feynman, R. P.; Leighton, R. B.; Sands, M. *The Feynman Lectures on Physics*; Addision-Wesley: Reading, MA, 1966; Vol. 1.

(25) To minimize confusion, it may be noted that in the most preferred FECA/X alloy, the X should be such that the lowest possible T_E corresponds to the lowest possible atomic percentage of this X in the FECA/X composition C_L. At the same time FECA of this FECA/X alloy should be such that T_L for this alloy is relatively high and hence the NW growth rate with this FECA is high. For example, Al/Si (12.2% at wt of Si) alloy with $T_E = 577$ °C should lead to higher Si NW growth rate than Au/Si (∼30% at. wt of Si) alloy with $T_E \approx 375$ °C.

(26) Novotny, C. J. *Appl. Phys. Lett.* **2005**, *87*, 203111.

(27) He, M.; Mohammad, S. N. *J. Vac. Sci. Technol., B* **2007**, *25*, 940.

(28) (a) Zou, J.; Paladugu, M.; Wang, H.; Auchterlonie, G. J.; Guo, Y.-N.; Kim, Y.; Gao, Q.; Joyce, H. J.; Hoe, H.; Jagadish, C. *Small* **2007**, *3*, 389. (b) See also: Kim, Y.; Joyce, H. J.; Gao, O.; Tan, H.; Jagadish, C.; Paradugu, M.; Zou, J.; Suvorova, A. A. *Nano Lett.* **2006**, *6*, 599.

(29) Shen, T. S.; Koch, C. C.; Wang, K. Y.; Quan, M. X.; Wang, J. T. *J. Mater. Sci.* **1997**, *32*, 3835.

(30) Increase in adatom crystallization on the substrate surface at higher temperatures has been documented by Reep, D. J.; Ghandhi, S. K. *J. Electrochem. Soc.* **1984**, *131*, 2697. Upward diffusion of adatoms via a nanowire sidewall may approximately be given by $\lambda_{SD}^2 = D_{S0}\tau_S \exp(\beta_{SD}E_{SD}/k_BT)$, which indicates that λ_{SD} and hence the upward adatom mobility via NW sidewalls decrease with increasing temperature.

(31) Dayeh, S. A.; Yu, E. T.; Wang, D. *Nano Lett* **2007**, *7*, 2486. In support of our model, Figures 7(a)–(c) of this article shows that nanowire length increases and nanowire tapering decreases with increasing temperature. It demonstrates also that nanowires exhibiting structure S6 (Figure 1) do exist, and that the largest NW lengths L_F (L_S) up to which the FECA (R_S species) can migrate via NW sidewalls do not exceed 1 μm. Excessively thick base of tapered nanowires as compared to the tips of these nanowires results probably due to upward diffusion of more numerous R_S species rather than due to the upward diffusion of possibly less numerous FECA atoms.

(32) Dick, K. A.; Deppert, K.; Martensson, T; Mandl, B.; Samuelson, L.; Seifert, W. *Nano Lett.* **2005**, *5*, 761.

(33) Kikkawa, J.; Ohno, Y.; Takeda, S. *Appl. Phys. Lett.* **2005**, *86*, 123109.

(34) Givargizov, E. I. *J. Cryst. Growth* **1975**, *31*, 20.

(35) Tan, T. Y.; Li, N.; Gosele, U. *Appl. Phys. Lett.* **2003**, *83*, 1199.

(36) Lim, S.-H.; Song, S.; Park, T.-S.; Yoon, E. *J. Vac. Sci. Technol., B* **2003**, *21*, 2388.

(37) Wilcoxon, J. P.; Samara, G. A. *Appl. Phys. Lett.* **1999**, *74*, 3164.

(38) Hu, J. Y.; Odom, T. W.; Lieber, C. M. *Acc. Chem. Res.* **1999**, *32*, 435.

NL072974W